

# Applicability of energy-based simplified evaluation on earthquake-induced slope displacements

Takaji Kokusho<sup>1</sup>

<sup>1</sup> Professor Emeritus, Chuo University, 46-5-1504 Senju-Asahicho, Adachiku, Tokyo, 120-0026, Japan.

## ABSTRACT

Simplified numerical analyses are conducted wherein the Newmark type slope model is shaken underneath by vertically propagating SH wave. Earthquake energy for slope sliding as energy difference between upward and downward waves is confirmed to balance with the energies associated with slope sliding. The residual slope displacements  $\delta_r$  are uniquely correlated with the energy irrespective of earthquake waves, indicating that  $\delta_r$  can be readily evaluated without using acceleration time-histories. The evaluation procedure has been developed using the analytical results and empirical formulas on wave energies. An example study for slope displacements of varying hypocenter distances during a M6.8 earthquake has shown a qualitative compatibility with a case history of road embankments.

**Keywords:** earthquake energy; slope failure; residual displacement; design chart

## 1 CONCEPT OF ENERGY-BASED METHOD

To evaluate seismic slope failures in terms of energy, an energy approach was previously proposed by the present author (Kokusho & Ishizawa 2007). In that method, earthquake induced slope displacement  $\delta_r$  for an infinitely long slope is expressed simply as;

$$\delta_r = E_{eq} / [\rho g D \tan(\phi - \theta)] \quad (1)$$

where,  $E_{eq}$  = earthquake energy for slope displacement in unit area,  $\rho g$  and  $D$  = unit weight and thickness of sliding soil,  $\phi$  = mobilized slope friction angle including cohesion, and  $\theta$  = slope angle. This equation was theoretically derived from energy balance in slope failure and demonstrated by model shaking table tests.

In applying Eq. (1) to slopes as schematically shown in Fig. 1, it is necessary to determine  $E_{eq}$  in field conditions by steps illustrated in Fig. 2. If a design earthquake motion is given at a base, the cumulative incident

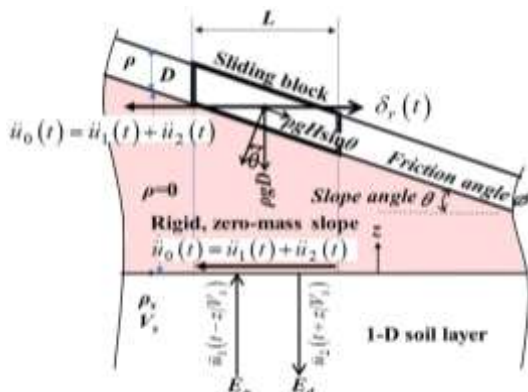


Fig.1. Infinitely long slope model with SH-wave.

energy  $E_{IP}$  per unit area is formulated (Kokusho 2017);

$$E_{IP} = (\rho_s V_s)_{base} \int [\dot{u}(t)]^2 dt \quad (2)$$

where,  $\dot{u}(t)$  = time history of upward-propagating particle velocity and  $(\rho_s V_s)_{base}$  = S-wave impedance at the base. If the earthquake motion is not available,  $E_{IP}$  may be roughly estimated at a seismological base layer corresponding to  $V_s = 3000$  m/s and  $\rho_s = 2.7$  t/m<sup>3</sup> as;

$$E_{IP} = E_0 / 4\pi R^2, \quad \log E_0 = 1.5M + 1.8 \quad (3)$$

where  $M$  = earthquake magnitude,  $R$  = hypocenter distance and  $E_0$  = total energy released based on Gutenberg (1956).

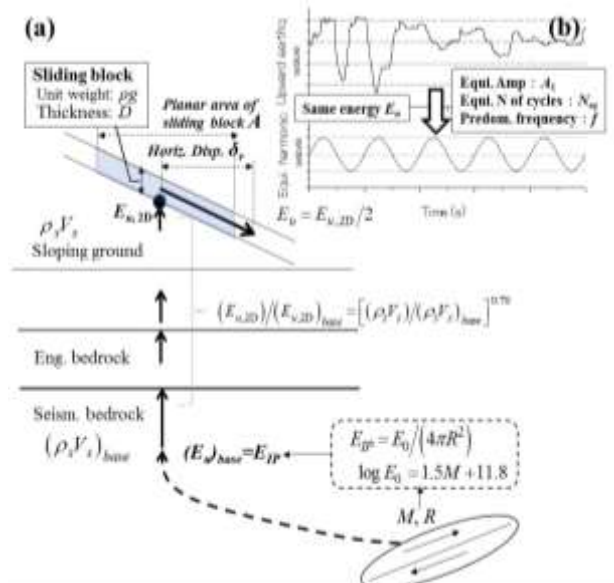


Fig. 2. Evaluation steps for input earthquake energy for energy-based slope failure evaluation.

Vertical array earthquake observation data demonstrated

that observed energies at seismological base layer  $E_{IP}$  are mostly compatible with Eq. (3). Total upward energy  $E_{u,2D}$  summed in 2 horizontal directions at a slope can be evaluated using another empirical formula based on strong motion vertical array records (Kokusho & Suzuki 2012) as;

$$E_{u,2D}/E_{IP} = \left[ (\rho_s V_s) / (\rho_s V_s)_{base} \right]^{0.7} \quad (4)$$

wherein  $\rho_s V_s$  and  $(\rho_s V_s)_{base}$  are S-wave impedance at the slope and base, respectively. The upward energy  $E_u$  in sloping direction should be  $E_u = E_{u,2D}/2$  averagely for a soil mass to slide in that direction according to previous study on earthquake observation (Kokusho et al. 2014).

## 2 ENERGY-BASED NEWMARK SLOPE MODEL

From the upward energy  $E_u$  beneath a potential sliding block, the earthquake energy  $E_{eq}$  for slope sliding is to be determined. For that goal, “Energy-based Newmark slope model” has been developed and shaken by SH-wave as depicted in Fig. 1, wherein a shaded virtual slope body of infinite rigidity and no mass is on the top of a horizontal layer where the SH-wave propagates vertically with S-wave velocity  $V_s$  as;

$$\ddot{u}(t, z) = \ddot{u}_1(t - z/V_s) + \ddot{u}_2(t + z/V_s) \quad (5)$$

At the surface of the horizontal layer ( $z=0$ );

$$\ddot{u}(t, 0) \equiv \ddot{u}_0(t) = \ddot{u}_1(t) + \ddot{u}_2(t) \quad (6)$$

Relative acceleration for the block sliding downslope in the Newmark model is expressed as (Sarma 1975);

$$\ddot{\delta}_r(t) = [\ddot{u}_0(t) - g \tan(\phi - \theta)] \cos(\phi - \theta) \cos \theta / \cos \phi \quad (7)$$

where  $\phi$ =friction angle between the block and slope and  $\theta$ =slope angle. In Eq. (7),  $\ddot{\delta}(t) > 0$  only if

$$\ddot{u}_0 - g \tan(\phi - \theta) > 0 \quad (8)$$

Horizontal force equilibrium of the block coupled with the SH-wave vibration transmitted through the virtual slope body can be expressed as;

$$\rho D (\ddot{u}_0(t) - \ddot{\delta}_r(t)) + G_s (\partial u(t, z) / \partial z) \Big|_{z=0} = 0 \quad (9)$$

where  $\ddot{u}_0(t) - \ddot{\delta}_r(t)$ =absolute acceleration of the block, and  $G_s = \rho_s V_s^2$ =shear stiffness. Substituting Eq. (5) into Eq. (9) yields the following basic equation.

$$\rho D (\ddot{u}_1(t) + \ddot{u}_2(t) - \ddot{\delta}_r(t)) = \rho_s V_s [\dot{u}_1(t) - \dot{u}_2(t)] \quad (10)$$

Eq. (10) together with Eqs. (7) and (8) can solve the slope system shown in Fig. 1 and its stationary harmonic response for angular frequency  $\omega$  can be obtained by substituting

$$\left. \begin{aligned} \ddot{u}_1(t) &= A_1 e^{i\omega t} & \dot{u}_1(t) &= (A_1 / i\omega) e^{i\omega t} \\ \ddot{u}_2(t) &= A_2 e^{i\omega t} & \dot{u}_2(t) &= (A_2 / i\omega) e^{i\omega t} \end{aligned} \right\} \quad (11)$$

into Eq. (10) as;

$$i \frac{\omega \rho D}{\rho_s V_s} [(A_1 + A_2) e^{i\omega t} - \ddot{\delta}_r(t)] = (A_1 - A_2) e^{i\omega t} \quad (12)$$

This indicates that  $\alpha = \omega \rho D / (\rho_s V_s)$  serves as a key pa-

rameter controlling Eq. (10), named here as impedance ratio, wherein  $\omega \rho D$  has the same dimension as  $\rho_s V_s$ . The nonlinear equation Eq. (10) for  $\ddot{\delta}(t) \neq 0$  has to be solved by numerical methods as explained below.

## 3 NUMERICAL ANALYSIS

Time integration of Eq. (10) together with Eqs. (7), (8) was implemented for a given input harmonic motion by using Wilson’s “ $\theta$ -method” with “ $\theta$ ” =1.4 to have a stable solution. Fig. 3 exemplifies the numerical results of the slope of  $\phi=35^\circ$ ,  $\theta=30^\circ$ ,  $D=10$  m,  $V_s=200$  m/s, and  $\rho = \rho_s = 1.8$  t/m<sup>3</sup>. As the input wave, a 10-cycle harmonic wave of frequency  $f=1.0$  Hz, was given wherein the amplitude increases from 0 to 100% linearly with time until 5<sup>th</sup> cycle followed by a constant amplitude  $A_1=2.0$  m/s<sup>2</sup> to avoid unfavorable effects of initial conditions. The slope starts to slide at 2<sup>nd</sup> cycle when  $\ddot{u}_0$  exceeds threshold (0.85 m/s<sup>2</sup>) defined by Eq. (8), and accumulates downward displacements. The bottom frame of Fig. 3 shows time-dependent variations of the associated energies. As the difference of energy  $E_{eq} = E_u - E_d$  and its sum with the gravitational energy  $E_{gr}$  accumulate with time,  $E_{gr} + E_{eq}$  is observed to be almost identical with the energy dissipating between the block and slope  $E_{ds}$ . This is compatible with the theoretical energy balance already discussed in previous papers by the author (e. g. Kokusho 2017).

Fig. 4(a) shows a slope displacement  $\delta_r$  versus earthquake energy  $E_{eq}$  relationship obtained as a stationary response per one cycle (in the 10<sup>th</sup> cycle of the tapered harmonic wave for different input accelerations). The calculations conducted for 3 different frequencies  $f=0.5 \sim 1.0$  Hz tend to give a unique correlation for the displacement  $\delta$  around 0.3 m or smaller though they tend to diverge with increasing  $\delta$  for higher  $f$  in particular presumably due to errors in the numerical

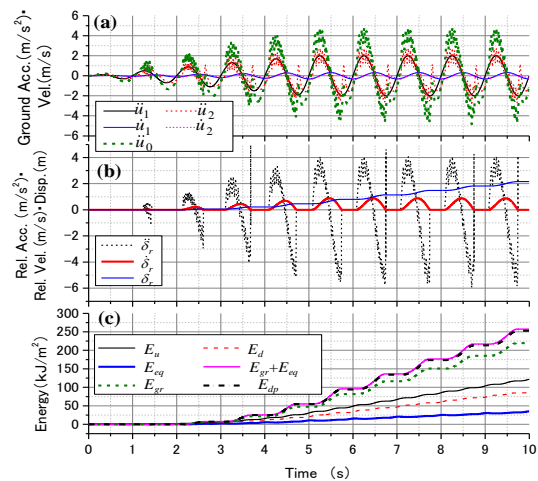


Fig. 3. Example analytical result of Energy-based Newmark slope model by a tapered harmonic wave ( $\phi=35^\circ$ ,  $\theta=30^\circ$ )

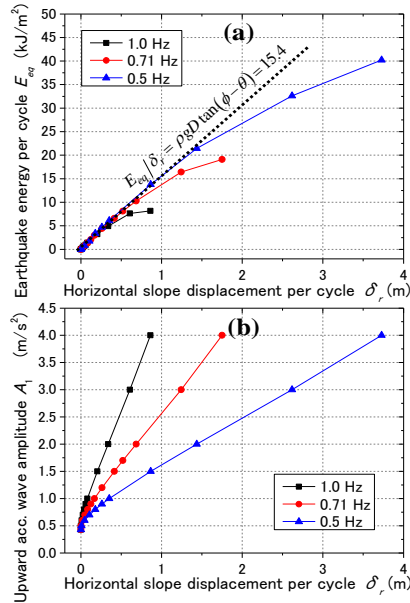


Fig. 4 Earthquake energy or upward acceleration amplitude versus horizontal slope displacement :  
(a)  $E_q \sim \delta$ , (b)  $A_1 \sim \delta$

analysis. Also note that for the small displacements the calculated results coincide with dashed straight line in the diagram representing Eq. (1) derived theoretically from a simple energy principle (Kokusho & Ishizawa 2007). In Fig. 4(b), the same calculated  $\delta$ -values are plotted versus horizontal slope accelerations ( $\approx 2A_1$ ) quite differently for three  $f$ -values, indicating that not the acceleration but the energy can serve as a unique indicator for slope displacements as already observed in previous model tests (Kokusho & Ishizawa 2007).

A series of analyses conducted for pertinent parameters,  $\phi = 35^\circ$ ,  $\theta = 20 \sim 30^\circ$ ,  $f = 0.5 \sim 1.0 \text{ Hz}$ ,  $D = 2.5 \sim 10 \text{ m}$ ,  $V_s = 150 \sim 300 \text{ m/s}$ , yield relationships between normalized energies  $E_{eq}/E_u/\alpha$  and  $E_u/N_{eq}/E_{u0}$  superposed in Fig. 5, where  $E_u$  and  $E_{eq}$  are upward and dissipated wave energies of an given earthquake,  $\alpha$  is impedance ratio involved in Eq. (12),  $N_{eq}$  = number of cycles of equivalent harmonic motion and  $E_{u0}$  is threshold upward energy for initiating slope sliding expressed as;

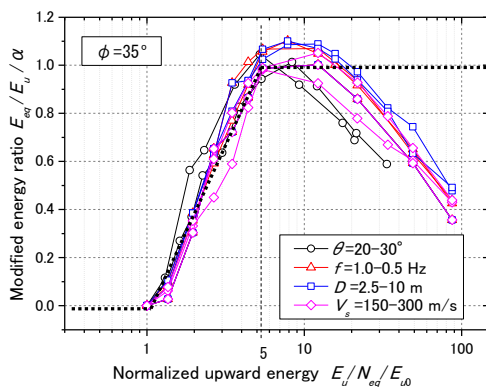


Fig. 5.  $E_{eq}/E_u/\alpha$  and  $E_u/N_{eq}/E_{u0}$  relationships numerically  
 $\phi$

$$E_{u0} = \frac{\pi \rho_s V_s}{4\omega^3} g^2 \tan^2(\phi - \theta) \quad (13)$$

for an equivalent harmonic motion with its angular frequency  $\omega = 2\pi f$ . Despite data dispersions due to calculation errors in the nonlinear analyses presumably, a trilinear dashed line may be drawn commonly for all the parameters considered here, yielding the following equation;

$$\left. \begin{aligned} E_u/N_{eq}/E_{u0} < 1.0: & \quad E_{eq}/E_u/\alpha = 0 \\ 1.0 < E_u/N_{eq}/E_{u0} < 5.0: & \quad E_{eq}/E_u/\alpha = 1.43 \log_{10}(E_u/N_{eq}/E_{u0}) \\ 5.0 \leq E_u/N_{eq}/E_{u0}: & \quad E_{eq}/E_u/\alpha = 1.0 \end{aligned} \right\} \quad (14)$$

Using earthquake energy  $E_{eq}$  here, the slope residual displacement  $\delta_r$  can be calculated from Eq. (1) using upward energy  $E_u$  depending on the impedance ratio  $\alpha$  and the threshold upward energy for sliding  $E_{u0}$ .

#### 4 EVALUATION EXAMPLE

Fig. 6(a) exemplifies a typical slope profile for conventional Newmark-type slope analysis along a circular slip surface, wherein the centroid O of soil block BCD slides to O' of B' C' D'. If the sliding displacement is not so large (less than a few meters for normal engineering design), the line OO' may be approximated parallel to the line BD with its angle  $\theta$ . Hence, it may be replaced in the energy method by a slide of a soil mass (horizontal length  $L$ ) on an infinitely long slope with the angle  $\theta$  as depicted in Fig. 6(b), wherein the mass  $M$  and planar slip area  $A = L \times 1$  are the same (exposed to the same upward wave energy) and the sliding soil thickness  $D = M/(\rho A)$ . In some cases, the slope profile in 6(b) may be directly employed for the analysis rather than replacing the circular slip analysis.

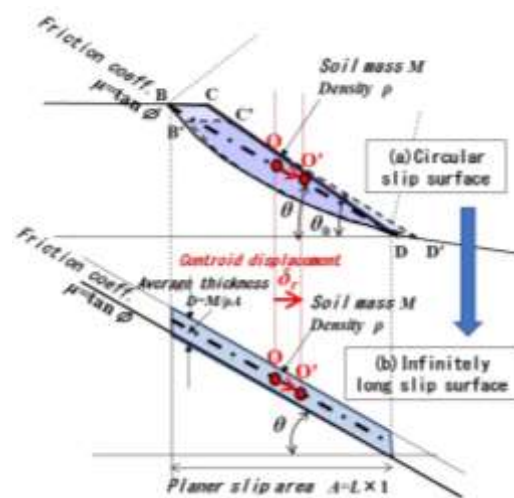


Fig. 6. Slope failures along circular surface (a) and straight surface (b) having the same soil mass and planar area



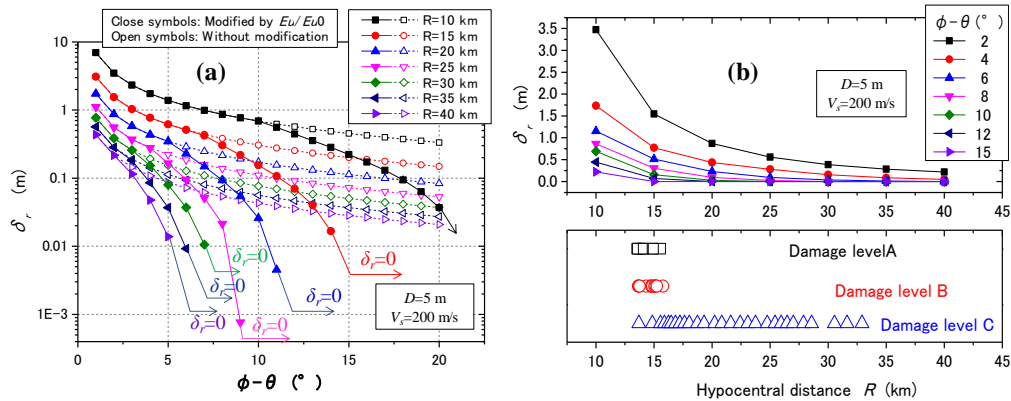


Fig. 7. Example evaluation of embankment slope displacements by M=6.8 earthquake: (a) displacements  $\delta_r$  versus  $\phi - \theta$  for varying hypocenter distance  $R$ , (b)  $\delta_r$  versus  $R$  compared with case history

In Fig. 7(a), slope displacements  $\delta_r$  for an earthquake of the magnitude  $M=6.8$  are plotted versus  $\phi - \theta$  for varying hypocenter distance  $R$ , wherein the earthquake energy was calculated by using Eqs. (3) and (4) as  $E_{IP}=796 \sim 49.7$  kJ/m<sup>2</sup> for  $R=10 \sim 40$  km. The earthquake motion is represented by a harmonic motion of equivalent number of cycles  $N_{eq}=9$  according to an empirical relationship (Idriss & Boulanger 2008) considering  $M=6.8$  and of equivalent frequency  $f=1.51$  Hz assuming PGA of  $M=6.8$  earthquake attenuating almost inversely proportional to  $R$  for  $R=10 \sim 40$  km (NIED 2004). This gives the wave energy beneath the slope per cycle (dividing  $E_{IP}$  by  $N_{eq}=9$ ) as  $E_u/N_{eq}=5.00 \sim 0.313$  kJ/m<sup>2</sup> for S-wave velocity  $V_s=200$  m/s using Eq. (4). By comparing this  $E_u/N_{eq}$ -value with the threshold energy  $E_{u0}$  in Eq. (13),  $E_{eq}$  for slope displacements can be determined by Eq. (14), leading to the evaluation of  $\delta_r$  in Eq. (1) assuming average thickness  $D=5.0$  m corresponding to circular slip. In Fig. 7(a), the curves of open symbols are originally plotted for  $E_{eq}/E_{u0}/\alpha=1.0$ . Then from these, close symbols are replotted depending on the kinks of  $E_u/E_{u0}$  at 1.0 and 5.0 as indicated in Eq. (14). Thus, co-seismic slope displacement can be evaluated by this method seamlessly from nonoccurrence ( $\delta_r=0$ ) to residual displacements (if occurred) without needs to design acceleration time histories.

In Fig. 7(b), the same displacements  $\delta_r$  are replotted versus  $R$  and compared with case history of the Kan-etsu highway embankment during 2004 Niigata Chuetsu earthquake ( $M=6.8$ ) where the damage level was classified into A (heavy), B (medium) to C (light) in slope sliding or road settlements (Kataoka et al. 2015). Although the comparison is still very much qualitative, the energy-based method seems to be able to properly evaluate slope behavior in terms of hypocenter distance and other pertinent slope parameters.

## 5 SUMMARY

Energy-based Newmark method has been developed

based on a series of numerical analyses where Newmark-type slope model is shaken by SH-wave propagation underneath. Occurrence/Nonoccurrence of slope failures and associated slope displacements can be evaluated directly from upward wave energy using pertinent slope parameters without using acceleration time histories. An example study by this method has indicated qualitative compatibility with embankment failure case history during a M6.8 earthquake in Japan.

## REFERENCES

- Kokusho, T. and Ishizawa, T. (2007). Energy approach to earthquake-induced slope failures and its implications, *Journal of Geotechnical and Geoenvironmental Engineering*, ASCE, Vol.133, No.7, 828-840.
- Kokusho, T. (2017). *Innovative Earthquake Soil Dynamics*, Chap.4, CRC publishers. P9.
- Gutenberg, B. (1956): The energy of earthquakes, *Quarterly Journal of the Geological Society of London*, Vol. CXII, No.455, 1-14.
- Newmark, N. M. (1965). Effects of earthquakes on dams and embankments, *Fifth Rankine Lecture, Geotechnique* Vol.15, 139-159.
- Kokusho, T. and Suzuki, T. (2012). Energy flow in shallow depth based on vertical array records during recent strong earthquakes (Supplement), *Soil Dynamics & Earthquake Engineering*, Vol. 42, 138-142.
- Kokusho, T., Koyanagi, T. and Yamada, T. (2014). Energy approach to seismically induced slope failure and its application to case histories –Supplement–, *Engineering Geology*, Elsevier, Vol. 181, 290–296.
- Sarma, S. K. (1975). Seismic stability of earth dams and embankments, *Geotechnique*, 25, No.4, 743-761.
- Idriss, I.M. and Boulanger, R. (2008): *Soil liquefaction during earthquakes*, Earthquake Engineering Research Institute, MNO-12, p.92.
- NIED: 2004 Niigata Chuetsu earthquake; motion and fault [http://cais.gsi.go.jp/KAIHOU/report/kaihou73/07\\_16.pdf](http://cais.gsi.go.jp/KAIHOU/report/kaihou73/07_16.pdf)
- Kataoka, S., Nagaya, K. and Matsumoto, K. (2015). Analysis on damage to road embankments caused by the Mid Niigata Prefecture earthquake 2004, *Journal of JSCE*, Vol. 71(4), 568-576.